# Numerical Study of Spectral Line Shapes in High-Density He Plasmas*)

Hayato KAWAZOME and Shinichi NAMBA[1)]

*Department of Information Engineering, National Institute of Technology, Kagawa College, 551 Kohda, Takuma-cho, Mitoyo 769-1192, Japan*

[1)]*Graduate School of Engineering, Hiroshima University, 1-4-1 Kagamiyama, Higashihirosima 739-8527, Japan*

(Received 30 November 2015 / Accepted 18 October 2016)

In order to determine the densities and temperatures in high-density helium plasmas by emission spectroscopy, a numerical study of He I spectral line shapes have been performed taking into account radiation trapping. A computational simulation code has been developed, consisting of two parts. The first part solves coupled rate equations to obtain population densities in each energy level of the He atom. The other describes the absorption rate, emission rate, and spectral line shapes by solving the equation of radiation transfer. In a homogeneous plasma, the calculated line profile has a central dip caused by photoabsorption by residual cold atoms. In addition, the results show that radiation trapping significantly alters the population dynamics. The population densities estimated from the intensity of the line profile considering the photoabsorption are lower by one order of magnitude than those without the photoabsorption. For application to a He arc plasma, the temporal evolution of this central dip is also examined as a preliminary calculation.



Keywords: spectral line shape, radiation transfer, coupled rate equations, He arc plasma

DOI: 10.1585/pfr.11.2401124

## 1. Introduction

To determine the electron temperature and density of a plasma, the spectral line intensity ratio of appropriate transitions can be employed with the experimental ratio being compared with a value calculated using a collisional-radiative (CR) model [1,2]. However, in high-density plasmas, such as atmospheric thermal plasmas or divertor plasmas of magnetically confined devices, the optical depth becomes significantly thick. For example, although atmospheric arc plasmas have been studied extensively sa a component of fundamental research into arcjet thrusters and atomic/molecular physics [3], it has been found that the radiation trapping of resonance transitions alters the population density distribution [4]. Consequently, we cannot apply the intensity ratio method to determine the temperatures and densities of such plasmas. In this study, therefore, the coupled rate equations for the He atom, incorporating radiation transport, are solved to derive the population densities and spectral line shapes of the resonance spectra. The optically thick transitions considered are He I 1s $^1$S - 2p $^1$P, 1s $^1$S - 3p $^1$P, and 1s $^1$S - 4p $^1$P and the respective wavelengths are 58.4, 53.7, and 52.2 nm. The simulation code developed, which directly solves the coupled rate equations, yields the time evolution of the population densities and the spectral line shapes.

In this paper, the coupled rate equations and the equation of radiative transfer are presented in Sec. 2. In Sec. 3, the plasma model and simulation code are described. The simulations for inhomogeneous and homogeneous plasmas are presented in Sec. 4. The final section provides summary.

## 2. Radiation Transfer and the Coupled Rate Equations

At a frequency $\nu$, the equation of radiation transfer corresponding to the transition $q \leftarrow p$ is given by

$$\mathrm{d}I_\nu = \{-k_\nu I_\nu + \eta_\nu\}\,\mathrm{d}x, \tag{1}$$

where $I_\nu$ is the radiance and $k_\nu$ and $\eta_\nu$ are the absorption coefficient and the emission coefficient, respectively. $x$ is the coordinate along the optical path [5]. In a spatially homogeneous medium, a formal solution of Eq. (1) is given by

$$I_\nu(x) = I_\nu(0)\exp(-k_\nu x) + \frac{\eta_\nu}{k_\nu}\left[1 - \exp(-k_\nu x)\right]. \tag{2}$$

Here, the absorption and emission coefficients are given by

$$k_\nu = \frac{h\nu}{4\pi}\left\{n_q B_{qp} P'(\nu) - n_p B_{pq} P(\nu)\right\}, \tag{3}$$

and

$$\eta_\nu = \frac{h\nu}{4\pi} n_p A_{pq} P(\nu), \tag{4}$$

*author's e-mail: kawazome@di.kagawa-nct.ac.jp*

*) This article is based on the presentation at the 25th International Toki Conference (ITC25).

respectively, where $A_{pq}$ is the Einstein $A$ coefficient from level $p$ to $q$; $B_{qp}$ and $B_{pq}$ are the Einstein $B$ coefficients for photoabsorption and induced emission, respectively; $h$ is the Planck constant; and $n_p$ is the population density of the level $p$. $P(\nu)$ and $P'(\nu)$ are the line profiles, normalized to 1, for emission and absorption, respectively. Assuming that $P(\nu)$ and $P'(\nu)$ have the same Gaussian shape, they are expressed as

$$P(\nu) = P'(\nu) = \frac{1}{\Delta\nu\sqrt{\pi}}\exp\left[-\left(\frac{\nu-\nu_0}{\Delta\nu}\right)^2\right], \tag{5}$$

where

$$\Delta\nu = \frac{\nu_0}{c}\sqrt{\frac{2k_BT}{m_{He}}}. \tag{6}$$

Here, $k_B$ is the Boltzmann constant, $T$ is the temperature of the emitting or absorbing neutral He atoms, $m_{He}$ is the mass of the He atom, $c$ is the speed of light and $\nu_0$ is the central frequency of the spectrum. The central frequencies of the spectra for the resonance transitions 1s $^1$S - 2p $^1$P, 1s $^1$S - 3p $^1$P, and 1s $^1$S - 4p $^1$P are $5.13\times10^{15}$ Hz, $5.58\times10^{15}$ Hz, and $5.74\times10^{15}$ Hz, respectively.

For the population density of level $p$, the coupled rate equations including radiation trapping are [6]

$$\begin{aligned}\frac{dn_p}{dt} = &-\Bigg\{\sum_{q\neq p}C_{pq}n_en_p + S_pn_en_p + \sum_{q<p}A_{pq}n_p \\ &+ \sum_{q>p}\int_{line}B_{pq}I_{qp}(\nu)n_pP'(\nu)d\nu + \sum_{q<p}\int_{line}B_{pq}I_{pq}(\nu)n_pP(\nu)d\nu\Bigg\} \\ &+ \Bigg\{\sum_{q\neq p}C_{qp}n_en_q + \sum_{q>p}A_{qp}n_q \\ &+ \sum_{q<p}\int_{line}B_{qp}I_{pq}(\nu)n_qP'(\nu)d\nu + \sum_{q>p}\int_{line}B_{qp}I_{qp}(\nu)n_qP(\nu)d\nu\Bigg\} \\ &+ \left(\alpha_pn_e + \beta_p + \beta_p^d\right)n_in_e,\end{aligned} \tag{7}$$

where $C_{pq}$ is the electron impact transition rate coefficient. $S_p$ is the ionization rate coefficient. $\alpha_p$, $\beta_p$, and $\beta_p^d$ are the rate coefficients for three-body, radiative, and dielectronic recombination, respectively. The fourth, fifth, eight, and the ninth terms on the right side in Eq. (7) represent the absorption rate for the outflow to upper levels, the induced emission rate for the outflow to lower levels, the absorption rate for the inflow from lower levels, and the induced emission rate for the inflow from upper levels, respectively.

# 3. The Plasma Model and Radiation Transport Simulation

In this study, numerical calculations of radiation transport in high-density He plasmas were performed. Figure 1 shows a schematic drawing of the plasma geometry. The plasma has a cylindrical shape and is divided into $(n+1)$ regions. The radius of the plasma cylinder is 0.25 cm and its cross section d$S$ is 0.196 cm$^{-2}$. The length of the plasma

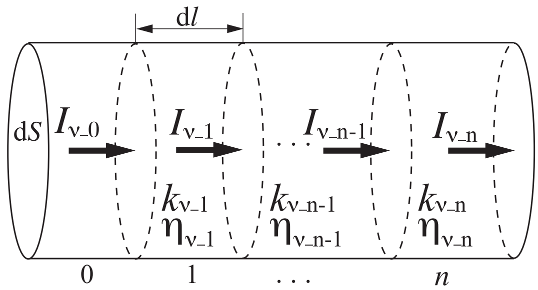


Fig. 1 A schematic drawing of the cylindrical plasma used in the radiation transport simulation. The plasma is divided into $(n+1)$ segments of length d$l$.

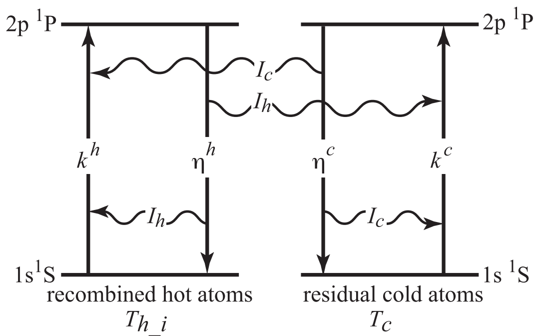


Fig. 2 Two photoabsorption processes for the 1s $^1$S - 2p $^1$P transition. The temperatures of the recombined hot atoms and the residual cold atoms are $T_{h\_i}$ and $T_c$, respectively. $k^h_{\nu\_i}$ and $k^c_{\nu\_i}$ are the absorption coefficients for the recombined hot atoms and the residual cold atoms, respectively. In the same manner as described above, for each temperature component, $\eta^h_{\nu\_i}$ and $\eta^c_{\nu\_i}$ are the emission coefficients and $I_h$ and $I_c$ are the radiance values.

cylinder $L$ is $L = (n+1)$ d$l$. Here d$l$ is the length of a single volume element. The mesh $i$ ($i = 0, 1, \cdots, n-1, n$) has electron temperature $T_{e\_i}$, electron density $n_{e\_i}$, absorption coefficient $k_{\nu\_i}$, and radiation coefficient $\eta_{\nu\_i}$. The ion density $n_{i\_i}$ is equivalent to the electron density $n_{e\_i}$, and the temperature of the recombined hot atoms $T_{h\_i}$, which are generated as a result of the recombination of helium ions, is set equal to the electron temperature. This assumption is justified in high-density thermal equilibrium plasmas. The density $n_c$ and temperature $T_c$ of the residual cold atoms are constant throughout the volume. Each value of the parameters is as determined in the center of the mesh. Figure 2 shows a schematic drawing of the photoabsorption processes for the 1s $^1$S - 2p $^1$P transition in this simulation. In the figure, $k^h_{\nu\_i}$ is the absorption coefficient of the recombined hot atoms and is calculated with $T_{h\_i}$. On the other hand, $k^c_{\nu\_i}$ is that for the residual cold atoms and is calculated with $T_c$. $I_h$ and $I_c$ are the radiance values from the recombined hot atoms and residual cold atoms, respectively. In the same way, $\eta^h_{\nu\_i}$ and $\eta^c_{\nu\_i}$ are emission coefficients for the recombined hot atoms and the residual cold atoms, respectively. For the other resonance transitions, similar procedures are also employed.

The algorithm used in the simulation code is divided into two sections: the coupled rate equations and the equation of radiation transfer. The computational scheme of the code is as follows:

(*a*) In each computational mesh, the time evolution of two sets of the coupled rate equations are solved. One of the coupled rate equations is solved with $n_{\mathrm{i}\_i}$, $n_{\mathrm{e}\_i}$, $T_{\mathrm{e}\_i}$, and $n_{\mathrm{h}}$ for the recombined hot atoms, and the other is solved with $n_{\mathrm{e}\_i}$, $T_{\mathrm{e}\_i}$, and $n_{\mathrm{c}}$ for the residual cold atoms. We then obtain the spatial profile of the population densities. The time step size d$t$ is $1.0 \times 10^{-12}$ s. At the first time step, the induced emission and absorption rates are zero because $I_{pq}$ values are zero. Whenever an increment in the time reaches the time step size for the equation of radiation transfer (which will be defined later), (*b*), (*c*), and (*d*) are carried out.

(*b*) Using the population densities obtained in (*a*), the absorption coefficient $k_{\nu\_i}$ and the emission coefficient $\eta_{\nu\_i}$ are calculated ($i = 1, 2, \dots n$). $k_{\nu\_i}$ is the sum of $k^{\mathrm{h}}_{\nu\_i}$ and $k^{\mathrm{c}}_{\nu\_i}$. $\eta_{\nu\_i}$ is also the sum of $\eta^{\mathrm{h}}_{\nu\_i}$ and $\eta^{n}_{\nu\_i}$.

(*c*) The line profile of $I_{\nu\_1}$ is calculated using Eq. (2), i.e.,

$$I_{\nu\_1}(\mathrm{d}l) = I_{\nu\_0} \exp(-k_{\nu\_1}\mathrm{d}l) + \frac{\eta_{\nu\_1}}{k_{\nu\_1}} \left[1 - \exp(-k_{\nu\_1}\mathrm{d}l)\right]. \tag{8}$$

Then, $I_{\nu\_i}$ is calculated using $I_{\nu\_i-1}$ ($i = 1, 2, \dots n$). $I_{\nu\_n}$ corresponds to the experimentally measured spectrum.

(*d*) Using the line profiles obtained in (*c*), the induced emission and absorption rates are calculated in each segment, and these values are used in the next time step.

(*e*) The processes described above are repeated iteratively until steady-state population densities are obtained (typical time : $10^{-5}$ s).

From the plasma geometry (see Fig. 1), the time period for the photons to travel from segment $i = 0$ to $i = n$ is $L/c$. However, in the high-density recombining plasma, a time step size of $1.0 \times 10^{-12}$ s is required to solve the coupled rate equations appropriately, because collisional processes such as three-body recombination and collisional de-excitation are very rapid phenomena. In this study, therefore, a time step size of $1.0 \times 10^{-12}$ s is used to calculate the coupled rate equations. On the other hand, for the equation of radiation transfer, the time step size is set to be greater than $L/c$ s. For example, in the case of $L = 5$ cm, $L/c$ is $1.67 \times 10^{-10}$ s and we use a time step size of $2.0 \times 10^{-10}$ s.

## 4. Numerical Results and Discussion

To investigate the effect of radiation trapping on the population density distribution and spectral line shape, we performed simulations for a plasma with a mesh count $n = 5$ and a plasma cylinder length of 5.0 cm. The temperature of the residual cold atoms was $T_{\mathrm{c}} = 0.026$ eV (300 K). The ion and electron densities were $n_{\mathrm{i}\_i} = n_{\mathrm{e}\_i} = 10^{14}$ cm$^{-3}$. The electron temperature was $T_{\mathrm{e}\_i} = 0.5$ eV. The spatial distributions of the electron temperature and the density were constant throughout the plasma. The time step size for the equation of radiation transfer was $2.0\times10^{-10}$ s. Figure 3 shows the spectral line profiles $I_{\nu\_5}$ (see Fig. 1) of the 1s $^1$S - 2p $^1$P transition at time $5.0\times10^{-5}$ s. The densities of the residual cold atoms were $10^{13}$, $10^{14}$, and $10^{15}$ cm$^{-3}$. In the calculation, a slit function is not considered. In Fig. 3, the peak heights are normalized. As is clearly seen, the profiles have a hollow shape, as the central frequency has the highest absorption probability. For the residual cold atoms of $10^{13}$, $10^{14}$, and $10^{15}$ cm$^{-3}$, the absorption coeffi-

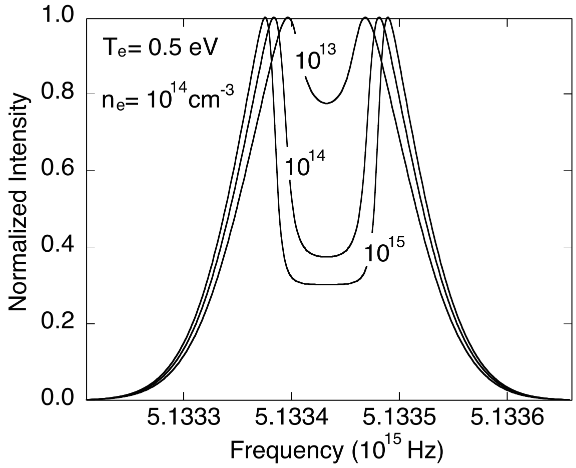


Fig. 3 Spectral line profiles of the transition 1s $^1$S - 2p $^1$P for the inhomogeneous plasmas. The electron temperature is 0.5 eV and the electron density and the ion density are $10^{14}$ cm$^{-3}$. The densities of the residual cold atoms are $10^{13}$, $10^{14}$, and $10^{15}$ cm$^{-3}$.

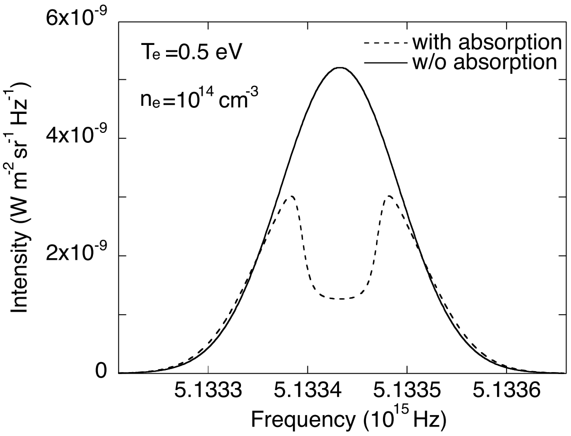


Fig. 4 1s $^1$S - 2p $^1$P line profile calculated with/without the effect of radiation trapping. The electron temperature is 0.5 eV and the density of the residual cold atoms is $10^{14}$ cm$^{-3}$.

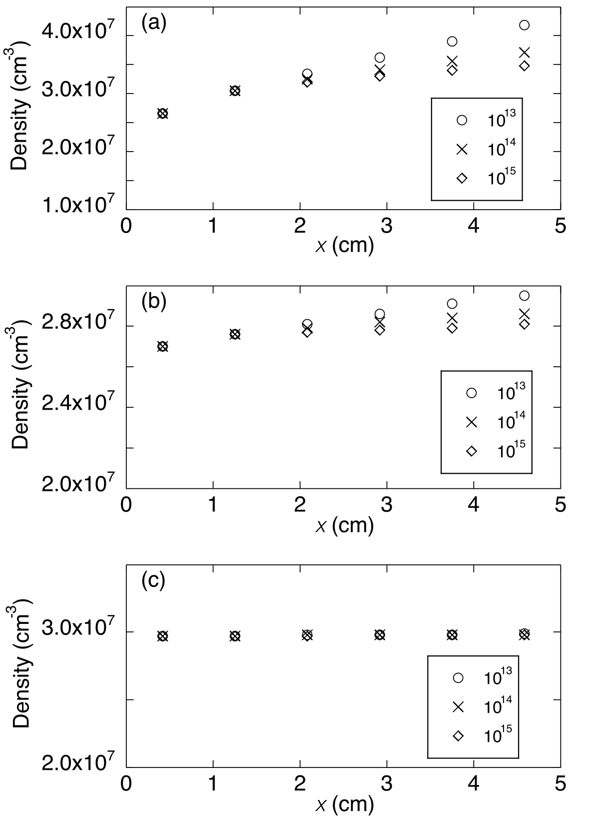


Fig. 5 Population density distributions of (a) 2p $^1$P, (b) 3p $^1$P, and (c) 4p $^1$P at an electron temperature of 0.5 eV. The densities of the residual cold atoms were $10^{13}$, $10^{14}$, and $10^{15}$ cm$^{-3}$.

cients $k^{\mathrm{c}}_{\nu_0}$ are $2.2 \times 10^2$, $2.2 \times 10^3$, and $2.2 \times 10^4$ m$^{-1}$, respectively, at the central frequency. For the recombined hot atoms, $k^{\mathrm{h}}_{\nu_0}$ is $2.1 \times 10$ m$^{-1}$ at the central frequency. The appearance of the central dip in the line profile indicates that the resonance line emitted by the recombined hot atoms is absorbed by the residual cold atoms. Thus, with higher densities, a deeper dip is observed. Figure 4 shows the 1s $^1$S - 2p $^1$P line profiles as calculated with/without accounting for radiation trapping. The density of the residual cold atoms was $10^{14}$ cm$^{-3}$. In Fig. 4, the estimated population densities of 2p $^1$P with and without the inclusion of photoabsorption are $6.0 \times 10^6$ and $2.7 \times 10^7$ cm$^{-3}$, respectively. Figure 5 plots the spatial distributions of the population densities of 2p $^1$P, 3p $^1$P and 4p $^1$P at time $5.0 \times 10^{-5}$ s. The densities of the residual cold atoms are $10^{13}$, $10^{14}$, were $10^{15}$ cm$^{-3}$. In the figure, the horizontal axis corresponds to the position relative to the origin (see Fig. 1). The population densities of 2p $^1$P and 3p $^1$P increase in proportion to the distance $x$. In the radiation transfer process, as the radiation goes through each mesh, $I_{\nu\_i}$ increases due to additional radiation as expressed by the radiation coefficient. The increase in the population density results from an increase in the absorption rate at each mesh. On the other hand, the population density of 4p $^1$P is almost constant throughout the plasma. The $A$ coefficient for the transitions of 1s $^1$S to 2p $^1$P, 3p $^1$P, and 4p $^1$P are $1.8 \times 10^9$, $5.6 \times 10^8$, and $2.4 \times 10^8$ s$^{-1}$, respectively. The $B$ coefficients for the photoabsorption from 1s $^1$S to 2p $^1$P, 3p $^1$P, and 4p $^1$P are $2.7 \times 10^{12}$, $6.6 \times 10^{11}$, and $2.6 \times 10^{11}$ J$^{-1}$ m$^2$ sr Hz, respectively. Because the $A$ coefficient of the 1s $^1$S - 4p $^1$P transition is smaller than that of the other transitions, the $B$ coefficient of the 1s $^1$S - 4p $^1$P transition has the lowest value among these transitions. In addition, in high-density plasmas, the electron impact transition plays a crucial role, and the outflow from 4p $^1$P into $n$p $^1$P ($n$ is the principal quantum number) increases. Thus, the effect of photoabsorption on the population density of 4p $^1$P is smaller. Further analysis of these excitation and deexcitation flows is necessary, which allows for a more detailed investigation.

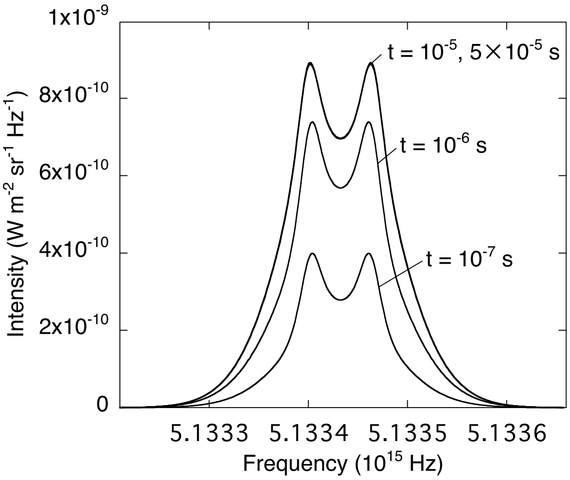


Fig. 6 Time evolution of the line profile for the 1s $^1$S - 2p $^1$P transition at various times.

Next, we show the preliminary result for the high-density He arc plasmas. The mesh number $n = 3$, and the length and radius of the plasma cylinder are 1.0 cm and 0.25 cm, respectively. The spatial profiles of the electron temperature and density are given by $T_{\mathrm{e}}(x) = T_{\mathrm{e0}}\{1 - (x/1.0)^2\}^2$ and $n_{\mathrm{e}}(x) = n_{\mathrm{e0}}\{1 - (x/1.0)^2\}^2$, respectively. Here, $T_{\mathrm{e0}}$ is 0.5 eV and $n_{\mathrm{e0}}$ is $10^{14}$ cm$^{-3}$. The density of the recombined hot atoms is $10^{12}$ cm$^{-3}$. The temperature and density of the residual cold atoms are set to be 0.026 eV and $10^{14}$ cm$^{-3}$, respectively. The ion density is $10^{14}$ cm$^{-3}$. The time step size for the equation of radiation transfer is $5.0 \times 10^{-11}$ s. Figure 6 shows the time evolution of the line profile for the 1s $^1$S - 2p $^1$P transition. The central dip can still be seen at early time. The He ions begin to recombine at $t = 0$, and the recombination flux causes an increase in the population density of 2p $^1$P. As a consequence, the central dip becomes clearer. At $1.0 \times 10^{-5}$ and $5.0 \times 10^{-5}$ s , the line profiles overlap with each other, as the population densities reached a steady state.

# 5. Summary

In order to investigate the effect of radiation trapping on the population density distributions and spectral line shapes in a low temperature and high-density He plasma, a numerical simulation code has been developed. The calculated line profiles show a central dip created by significant photoabsorption by residual cold atoms. By comparing the results with and without photoabsorption, it has been shown that the population densities estimated from the intensity of the line profile when including photoabsorption were lower by an one order of magnitude than when photoabsorption was not included. Moreover, radiation trapping significantly alters the population dynamics. For a high-density He arc plasma, the preliminary result of the time evolution of the line profile clearly shows the growth of a central dip. In future work, we plan to compare experimental results with our numerical simulations.

[1] B. Schweer, G. Mank, A. Pospieszczyk, B. Brosda and B. Pohlmeyer, J. Nucl. Mater. **196-198**, 174 (1992).

[2] L. Garraro, G.D. Pol, M.E. Puiatti, F. Sattin, P. Scarin and M. Valisa, Plasma. Phys. Control. Fusion **42**, 1 (2000).

[3] S. Namba, N. Yashio, K. Kozue *et al.*, Jpn. J. Appl. Phys. **48**, 116005 (2009).

[4] Y. Iida, S. Kado, A. Okamoto, S. Kajita, T. Shikama, D. Yamasaki and S. Tanaka, J. Plasma Fusion Res. SERIES **7**, 123 (2006).

[5] T. Fujimoto, *Plasma spectroscopy* (Oxford University Press, Oxford, 2004) p. 240.

[6] S. Kado, M. Goto *et al.*, J. Plasma Fusion Res. **86**, 631 (2010) (in Japanease).